RSC Advances

PAPER

View Article Online
View Journal | View Issue

Cite this: *RSC Adv.*, 2023, **13**, 19106

New insights into defects and magnetic interactions inducing lattice disordering in $Co_2Fe_{0.5}Cr_{0.5}Al$

Ravi Kumar Yadav,[ac] R. Govindaraj, *[ac] K. Vinod,[ac] T. Sreepriya[bc] and R. Mythili[bc]

Atomic scale understanding of defect induced magnetic interactions resulting in lattice disordering has been deduced in a detailed manner for the first time in $Co_2Fe_{0.5}Cr_{0.5}Al$ based on Mössbauer spectroscopic studies and compared with the results obtained in $Co_2Fe_{0.8}Cr_{0.2}Al$ and Co_2FeAl. An interesting linear correlation between valence electron concentration and the mean hyperfine fields at Fe sites in Co_2FeAl based compounds has been deduced which is observed to exhibit different slopes with the substitution of Cr. This study elucidates an important role of the manifestation of the magnetic interactions especially between Fe, Co and Cr atoms leading to significant changes in the concentration and specific types of defects selectively produced in $Co_2Fe_{0.5}Cr_{0.5}Al$ as compared with that of $Co_2Fe_{0.8}Cr_{0.2}Al$ subjected to similar non-equilibrium treatments in this study. Further, for the first time this study elucidates the striking correlation of the effective value of the hyperfine field with the degree of ordering/disordering of the lattice with the Fe atoms associated with ordered sites experiencing a much higher value of the hyperfine field as compared to that of the disordered sites. This study also proposes optimal annealing treatment for the recovery of defects in $Co_2Fe_{0.5}Cr_{0.5}Al$, which would be of significant importance in these spintronic materials.

Received 30th December 2022
Accepted 31st May 2023

DOI: 10.1039/d2ra08318c

rsc.li/rsc-advances

1. Introduction

Half metallic ferromagnets are being extensively investigated for spintronics studies for various device applications including magnetic tunnel junctions.[1–4] Cobalt based Heusler compounds are quite important having a high magnetic moment and Curie temperature up to 1300 K.[5–7] It is important that any material of interest for spintronic applications exhibits a high value of spin polarization which is defined as $[N(\uparrow) - N(\downarrow)]/[N(\uparrow) + N(\downarrow)]$, where $N(\uparrow)$ and $N(\downarrow)$ denote the number of electrons at the Fermi level in the spin up and spin down band respectively.[8–10] These quantities are weighted by powers of Fermi velocity $\mathbf{V}_{F\uparrow}$ and $\mathbf{V}_{F\downarrow}$ to account for the mechanism involved in measuring polarization based on the technique employed such as photoemission,[11] point contact magnetoresistance,[12] tunnelling magneto resistance[13,14] and Andreev reflection.[15,16] Apart from lattice disordering/ordering which dictates mainly the spin polarization of the Heusler compound concerned, properties such as oxidation free surface, well reduced roughness of the interface critically affect the values of spin polarization and tunnelling magneto resistance respectively. The lattice order/disorder hence plays a dominant role intrinsically dictating the spin polarization properties of the spintronic material of interest.[7,17–20] In the case of Co_2FeAl, against the theoretical prediction of half metallicity, only the maximum value of 60% of spin polarization has been reported in a thin film of Co_2FeAl.[21] Hence from the bulk structural point of view the effect of lattice disorder is the most important factor which dictates the spintronic properties.

It has been reported theoretically based on band structure computation that in Co_2CrAl and in $Co_2Fe_{(1-x)}Cr_xAl$ for low value of x having $L2_1$ ordering and B_2 type of disordering exhibit half metallic type of band structure.[22–25] It has been demonstrated experimentally that the compound $Co_2Fe_{0.6}Cr_{0.4}Al$ exhibits high value of tunnelling magneto resistance close to 19% at 300 K.[26] Though the value of spin polarization is high, as compared to the expected theoretical value of 100% it is quite low. This means that the lattice disordering might be playing a dominant role in these compounds composed of both Fe and Cr occupying Y sites. It is also important to understand as to how the magnetic interactions between Fe–Cr affect the lattice ordering/disordering. This study would focus on the aspects of defects and disordering in $Co_2Fe_{0.5}Cr_{0.5}Al$ in terms of the local structure and magnetic properties deduced at Fe sites. Ordered and possible disordered configurations of the system $Co_2Fe_{0.5}Cr_{0.5}Al$ are shown schematically in Fig. 1. In the presence of the disordering of the lattice half metallicity is likely to get lost

[a]*Materials Science Group, Indira Gandhi Centre for Atomic Research, Kalpakkam 603102, Tamilnadu, India. E-mail: govind@igcar.gov.in*

[b]*Metallurgy and Materials Group, Indira Gandhi Centre for Atomic Research, Kalpakkam 603102, Tamilnadu, India*

[c]*Indira Gandhi Centre for Atomic Research, A CI of Homi Bhabha National Institute, Kalpakkam 603102, Tamilnadu, India*

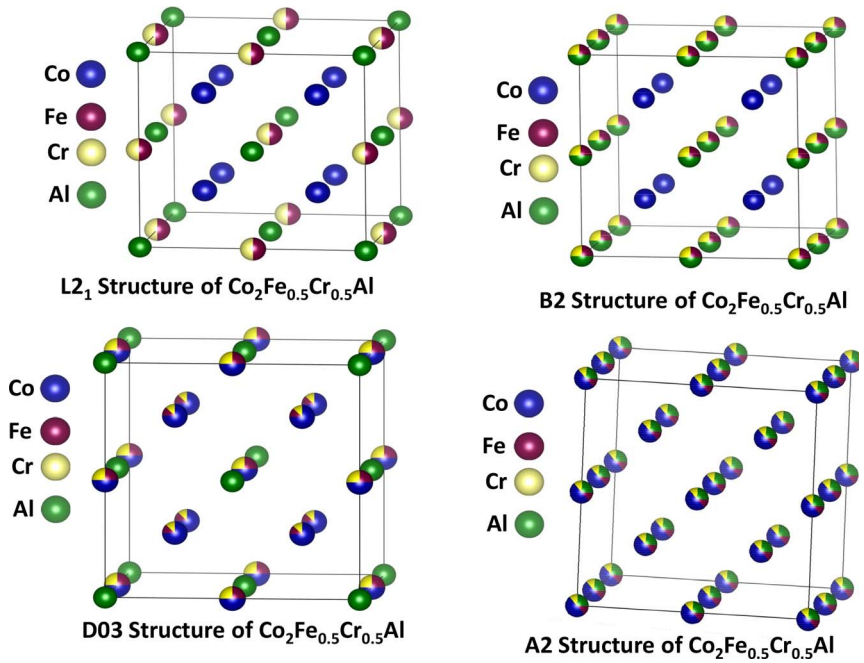

Fig. 1 Schematic shows $L2_1$ ordered $Co_2Fe_{0.5}Cr_{0.5}Al$ occupying Wyckoff positions 8c (1/4, 1/4,1/4) by Co, 4b (1/2,1/2,1/2) by Fe/Cr with equal probability and 4a (0,0,0) by Al atoms. Also shown are the disordered structures in the full Heusler compound $Co_2Fe_{0.5}Cr_{0.5}Al$ such as B_2, $D0_3$ and A_2 having (Fe,Cr)/Al, Co/(Fe,Cr) and Co/(Fe,Cr)/Al antisite disordering respectively as illustrated in the schematic.

leading to a drastic reduction in spin polarization. Because of the fact that the atomic number of Co, Cr and Fe are very close by it would be very difficult to deduce the degree of ordering or disordering of the lattice based on the results of X-ray diffraction based techniques. Dark field image analysis based on TEM studies carried out in $Co_2Cr_{0.6}Fe_{0.4}Al$ has shown the presence of A_2 phase enriched with Cr and depleted with Co atoms.[27] Based on the three dimensional atom probe microanalysis it was shown that even Fe and Al atoms were rejected from A_2 phase.[27] Hence $L2_1$ and A_2 phases shift to Co rich and Cr rich sides as predicted based on thermo dynamical computation. X-ray based scattering/absorption techniques would not lead to unambiguous understanding of the ordering/disordering of the lattice which mainly critically affects the spin polarization and hence spintronic properties. On the other hand experimental techniques which could simultaneously result in a good understanding of local structure and magnetic fields at specific sites in the matrix concerned might be powerful to study the lattice ordering and disordering which in turn mainly dictate the spin polarization properties.

The present work is motivated at studying mainly the lattice ordering/disordering induced due to quenching treatment in the compound $Co_2Fe_{0.5}Cr_{0.5}Al$ in order to mainly elucidate as to how the lattice defects get modified or manifested due to enhanced magnetic interactions between Fe and Cr atoms. This means that the present study is intended to understand the effect of defects which is likely to get modified appreciably in the presence of Fe–Cr interactions on the B_2 type of disordering. Results as obtained in this study will also be compared with that of Co_2FeAl doped with Cr of lower concentration Hence in this study the lattice disordering induced due to quenching has

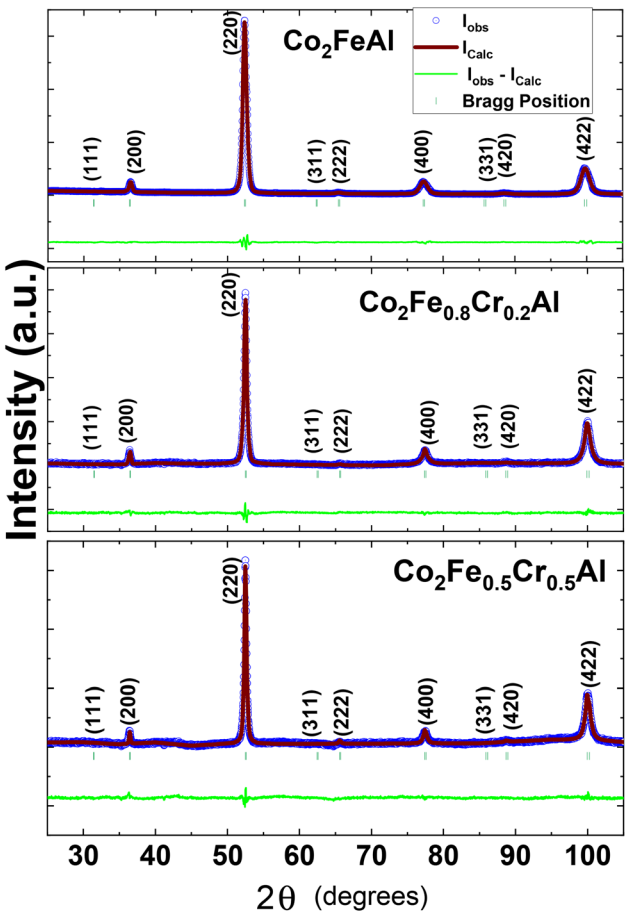

Fig. 2 Rietveld refined XRD patterns as obtained in Co_2FeAl, $Co_2Fe_{0.8}Cr_{0.2}Al$ and $Co_2Fe_{0.5}Cr_{0.5}Al$ using Co-K_α X-ray source.

Table 1 Results of the Rietveld refinement of XRD patterns

Sample	Lattice parameter (Å)	R_{wp} (%)	χ^2
Co_2FeAl	5.72 (5)	7.13	1.59
$Co_2Fe_{0.8}Cr_{0.2}Al$	5.72 (1)	7.81	1.62
$Co_2Fe_{0.5}Cr_{0.5}Al$	5.72 (3)	6.57	1.46

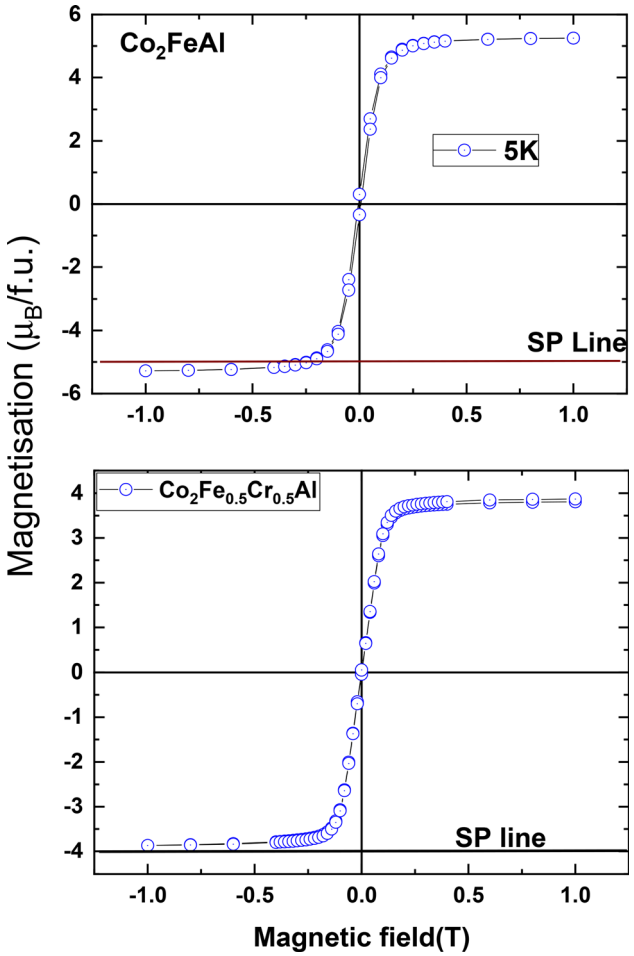

Fig. 3 Variation of magnetization with the applied magnetic field in the case of Co_2FeAl and $Co_2Fe_{0.5}Cr_{0.5}Al$. Line is drawn for each of the above systems at the value of the magnetization deduced based on the Slater–Pauling (SP) rule.

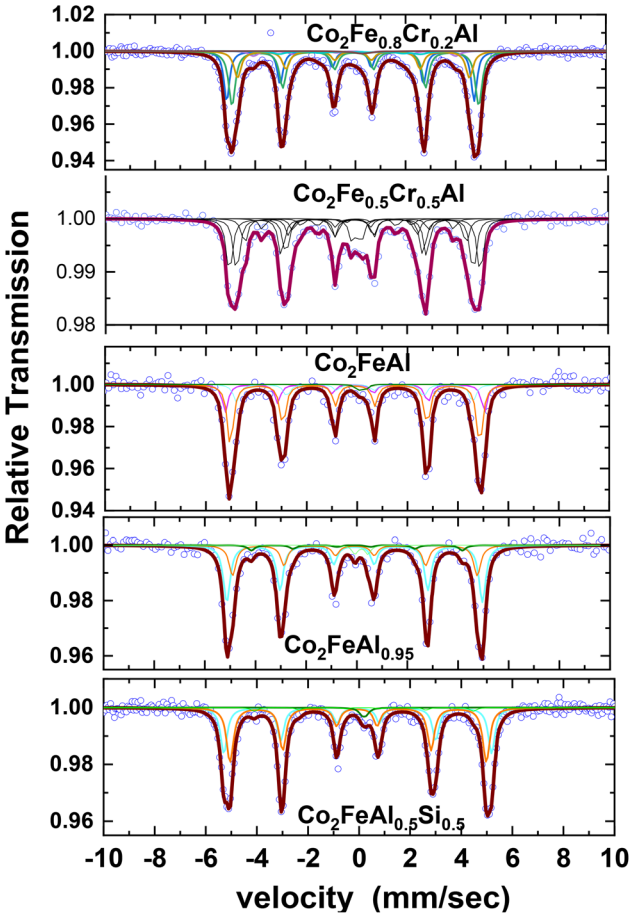

Fig. 4 Mössbauer spectra as obtained in $Co_2Fe_{0.8}Cr_{0.2}Al$, $Co_2Fe_{0.5}Cr_{0.5}Al$, Co_2FeAl, $Co_2FeAl_{0.95}$ and $Co_2FeAl_{0.5}Si_{0.5}$.

been investigated in a detailed manner based on isochronal annealing studies in the quenched $Co_2Fe_{0.5}Cr_{0.5}Al$ by means of deducing local structure and magnetic properties at Fe sites using ^{57}Fe based Mössbauer spectroscopy.

2. Experimental details

$Co_2Fe_{0.5}Cr_{0.5}Al$ samples were prepared by the arc melting of Co, Fe, Cr and Al from Alfa Aesar with the purity of each of the constituent to be close to 99.99% taken in a stoichiometric ratio in ultra-high pure Ar atmosphere. In the process of arc melting care is taken to re melt the sample a several times after flipping to ensure a good homogenization of the melted alloy. In order to deduce the role of Cr, another alloy of stoichiometry $Co_2Fe_{0.8}Cr_{0.2}Al$ has also been prepared similarly by arc melting.

Bulk structural characterization of the as melted sample has been carried out based on X-ray diffraction studies using Inel Equinox 2000 diffractometer with Co-K_α source. Full Prof Suite[28] has been utilised for Rietveld analysis of powder X-ray diffraction patterns. Bulk magnetization studies have been carried out using Cryogenic Ltd make Vibrating sample magnetometer (VSM). Mössbauer studies were carried out with the spectrometer operated in transmission geometry and in constant acceleration mode using ^{57}Co source of activity of 50 mCi dispersed in Rh matrix. Mössbauer spectra were fitted with a Lorentzian line shape to obtain the hyperfine parameters as experienced by different relative fractions of Fe atoms such as isomer shift (δ) and quadrupole splitting (Δ) and the hyperfine fields (B_{hf}). Values of the isomer shifts are reported with respect to that of α-Fe foil. The line width of the spectrum corresponding to alpha-Fe foil is deduced as 0.24 mm s^{-1}.

As the main focus of this work is to study the defects induced disordering, $Co_2Fe_{0.5}Cr_{0.5}Al$ are subjected to selective quenching treatments at temperatures of interest at a partial pressure

Table 2 Hyperfine parameters as deduced at Fe sites in pristine and suitably substituted Co_2FeAl

Sample treatment	(i)	δ_i (mm s^{-1})	Δ_i (mm s^{-1})	B_{hf} (T)	f_i
As arc melted Co_2FeAl	1	0.02 ± 0.01	0.06 ± 0.03	31.61 ± 0.05	0.32
	2	0.03 ± 0.01	0.02 ± 0.01	30.06 ± 0.05	0.34
	3	0.03 ± 0.01	0.04 ± 0.01	29.44 ± 0.04	0.31
	4	0.26 ± 0.01	0.69 ± 0.05	0	0.03
As arc melted $Co_2FeAl_{0.95}$	1	0.02 ± 0.01	0.04 ± 0.01	32.15 ± 0.04	0.13
	2	0.03 ± 0.01	0.04 ± 0.01	31.11 ± 0.02	0.43
	3	0.04 ± 0.02	0.03 ± 0.01	29.89 ± 0.03	0.33
	4	0.25 ± 0.01	0.42 ± 0.03	0	0.03
	5	0.07 ± 0.01	0.10 ± 0.03	25.05 ± 0.06	0.08
Co_2FeAl subjected to quenching from 1273 K to 77 K	1	0.01 ± 0.01	0.09 ± 0.005	32.07 ± 0.03	0.13
	2	0.03 ± 0.002	0.01 ± 0.002	30.83 ± 0.05	0.43
	3	0.03 ± 0.07	0.01 ± 0.002	29.53 ± 0.04	0.34
	4	0.22 ± 0.01	0.62 ± 0.03	0	0.03
	5	0.2 ± 0.03	0.14 ± 0.02	22.5 ± 0.06	0.07
Quenched Co_2FeAl annealed at 773 K/4 h	1	0.03 ± 0.01	0.02 ± 0.01	31.66 ± 0.06	0.34
	2	0.03 ± 0.01	−0.03 ± 0.01	30.53 ± 0.05	0.47
	3	0.03 ± 0.01	0.04 ± 0.02	28.9 ± 0.07	0.16
	4	0.14 ± 0.01	0.22 ± 0.03	0	0.03
$Co_2FeAl_{0.5}Si_{0.5}$	1	0.08 ± 0.002	0.05 ± 0.01	32.48 ± 0.05	0.41
	2	0.06 ± 0.001	0.05 ± 0.01	31.09 ± 0.02	0.52
	3	0.28 ± 0.03	0.15 ± 0.02	26.6 ± 0.05	0.04
	4	0.32 ± 0.04	0.17 ± 0.01	0	0.03
$Co_2Fe_{0.8}Cr_{0.2}Al$	1	−0.06 ± 0.01	−0.06 ± 0.01	30.64 ± 0.05	0.24
	2	0.09 ± 0.01	0.05 ± 0.01	30.50 ± 0.05	0.38
	3	0.04 ± 0.03	0.09 ± 0.05	25.05 ± 0.20	0.06
	4	0.03 ± 0.01	0.03 ± 0.01	28.7 ± 0.10	0.21
	5	0.13 ± 0.05	−0.47 ± 0.08	17.5 ± 0.31	0.08
	6	0.39 ± 0.06	0.18 ± 0.04	0	0.03
$Co_2Fe_{0.8}Cr_{0.2}Al$-1073 K-2 h-Q	1	0.16 ± 0.02	0.02 ± 0.01	28.24 ± 0.16	0.13
	2	−0.02 ± 0.01	−0.14 ± 0.02	30.90 ± 0.06	0.27
	3	0.06 ± 0.01	0.13 ± 0.02	30.75 ± 0.06	0.31
	4	0.22 ± 0.02	0.30 ± 0.04	0	0.05
	5	−0.03 ± 0.02	−0.08 ± 0.03	28.13 ± 0.14	0.14
	6	0.41 ± 0.09	0.38 ± 0.14	26.04 ± 0.68	0.05
	7	0.35 ± 0.04	0.16 ± 0.07	19.5 ± 0.30	0.05
$Co_2Fe_{0.5}Cr_{0.5}Al$	1	−0.07 ± 0.01	−0.03 ± 0.02	30.35 ± 0.11	0.27
	2	0.11 ± 0.02	0.05 ± 0.02	26.83 ± 0.15	0.16
	3	0.38 ± 0.04	0.28 ± 0.08	21.09 ± 0.28	0.12
	4	0.24 ± 0.02	0.34 ± 0.03	0	0.09
	5	0.06 ± 0.01	0.05 ± 0.02	28.70 ± 0.11	0.30
	6	0.12 ± 0.04	0.18 ± 0.08	7.45 ± 0.25	0.06

of 10^{-6} mbar. Towards studying the possible recovery of defects these samples are subjected to selective annealing treatments as will be discussed with respect to each case of study. Mössbauer studies have been carried out at room temperature. The results obtained in $Co_2Fe_{0.5}Cr_{0.5}Al$ are compared with that of $Co_2Fe_{0.8}Cr_{0.2}Al$ subjected to quenching.

3. Results and discussion

Rietveld refined X-ray diffraction (XRD) patterns as obtained using Co-K_α source in $Co_2Fe_{0.8}Cr_{0.2}Al$ and $Co_2Fe_{0.5}Cr_{0.5}Al$ (*cf.* Fig. 2) are compared with that of Co_2FeAl. Almost all the patterns are looking similar and showing the peaks in terms of (*hkl*) positions as (200), (220), (400) and (422). The (*hkl*) indices of the XRD patterns have been extracted using crystallographic information files of ICSD database code 57607. The chemical composition (in at%) of Co, Fe and Al in Co_2FeAl was 50.2 ± 0.4%, 24.3 ± 0.9% and 25.4 ± 1.2% respectively consistent with the stoichiometry. In the case of $Co_2Fe_{0.8}Cr_{0.2}Al$ the composition of Co,Fe,Cr and Al (in at%) were deduced as 49.7 ± 0.6%, 20.2 ± 0.8%, 5.0 ± 1.2% and 25.1 ± 1.6% respectively pointing to the correctness of the stoichiometry. Similarly commensurate with the stoichiometry of $Co_2Fe_{0.5}Cr_{0.5}Al$, the composition of Co,Fe,Cr and Al (in at%) were deduced as 50.6 ± 0.7%, 12.5 ± 0.8, 12.1 ± 1.1 and 24.8 ± 1.4%. Absence of the peak corresponding to the (*hkl*) values at (111) in XRD patterns implies the absence of $L2_1$ ordering in all these systems. While the presence of peak at (200) implies the occurrence of B_2 type of disordering in these systems though the intensity of (200) is quite less as compared to that of the most intense peak. Initial crystallographic parameters have been obtained from ICSD code file 57607 for the Rietveld analysis of XRD patterns. In case of $L2_1$ structure (space group no. 225) which is the most ordered structure for Heusler compound $Co_2Fe_{0.5}Cr_{0.5}Al$, in which 4a

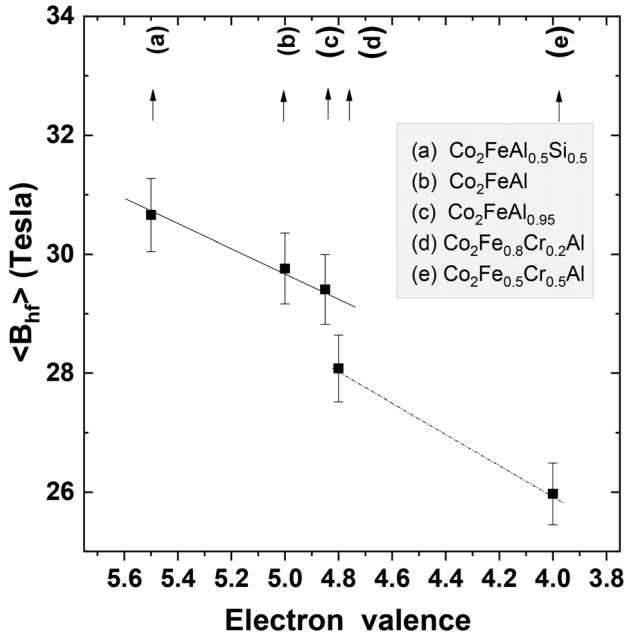

Fig. 5 Variation of the value of the mean hyperfine field with valence for different Co based Heusler compounds mentioned as (a–e).

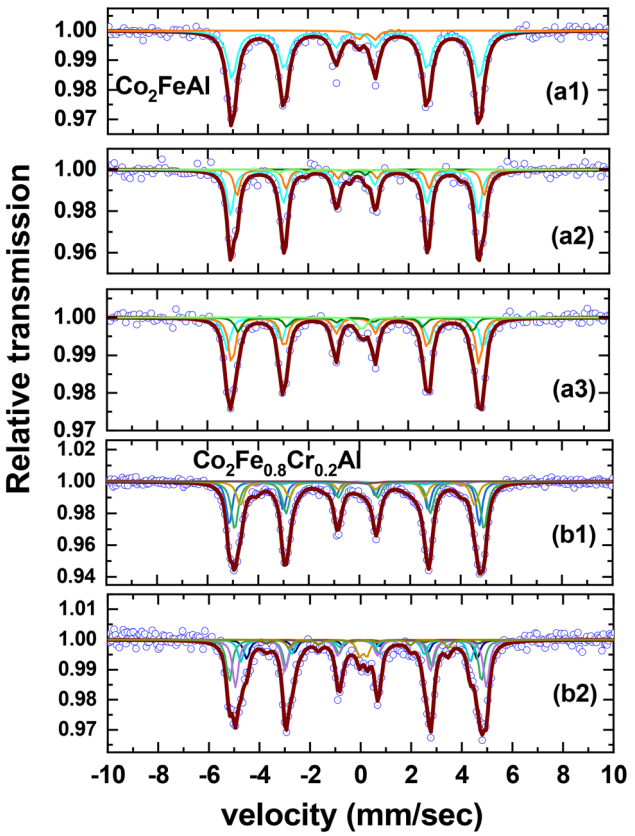

Fig. 6 Mössbauer spectra (MS) obtained in Co_2FeAl (a1) as melted (a2) subsequent to quenching at 1073 K and (a3) annealed at 673 K while (b1) and (b2) refer to MS spectra obtained in as melted and quenched $Co_2Fe_{0.8}Cr_{0.2}Al$.

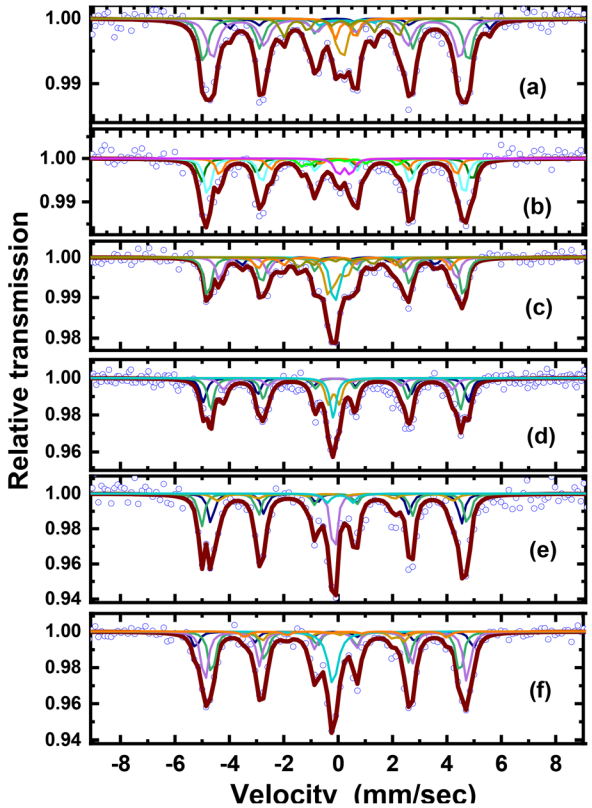

Fig. 7 Mössbauer spectra as obtained in $Co_2Fe_{0.5}Cr_{0.5}Al$ (a) as melted (b) with mag field (c) 1073 K 2 h quenched (d) 1073 K 2 h quenched + annealing at 573 K 2 h (e) sample (d) annealed at 673 K 2 h (f) sample (e) annealed at 723 K for 2 h.

and 8c sites are occupied by Al and Co atoms respectively with occupancy factor (occ) of 100%, whereas the 4b sites are occupied by Fe and Cr atoms with the occupancy factor of 50% for each. Since in all the experimental powder XRD patterns of all samples (200) peak is present and (100) peak is absent (*cf.* Fig. 2), therefore the Rietveld analysis has been performed considering the significant presence of B_2 type of disorder in all the patterns. In case of B_2 disorder, atoms occupying 4a & 4b sites have equal probability to occupy these sites 4a & 4b sites as shown in Fig. 1. By means of taking care of the overall stoichiometry of the compounds with the properly chosen site occupancy factors the absence of (111) peak in the XRD patterns is deduced. Results of Rietveld refinement in terms of the deduced lattice parameters, weighted-profile *R* factor[29] R_{wp} and χ^2 have been listed in Table 1. Similar results of Rietveld analysis have been reported in some of the different Heusler systems.[5,30] Absence of $L2_1$ ordering accompanied by a decrease in (200) peak could also be caused by the presence of A_2 type of disordering similar to the results as have been elucidated in the case of Co_2FeAl based on the results of Mössbauer spectroscopy.

Result corresponding to the bulk magnetization in $Co_2Fe_{0.5}Cr_{0.5}Al$ is compared with that of Co_2FeAl as shown in Fig. 3. The value of the saturation magnetization is deduced as 3.85 μ_B FU^{-1} in the case of $Co_2Fe_{0.5}Cr_{0.5}Al$ using vibration sample magnetometer. The observed value is less than the expected

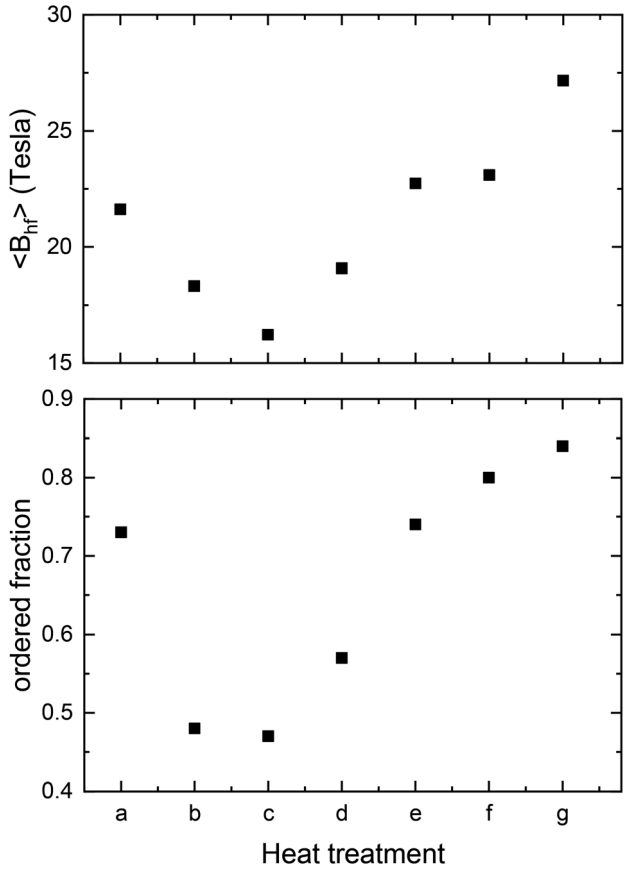

Fig. 8 Based on the results of quenching studies carried out in $Co_2Fe_{0.5}Cr_{0.5}Al$ an interesting correlation between the magnitudes of the ordered fractions is observed with respect to the value of the mean hyperfine field. Different heat treatments (a–g) are referred to Table 3.

value of 4 μ_B FU^{-1} (*(i.e.)* $(18 + 4 + 3 + 3) - 24 = 4$ μ_B FU^{-1}) by about 4.4% based on the Slater–Pauling rule. On the other hand it is seen that in the case of Co_2FeAl the observed value of saturation magnetization is 5.25 μ_B FU^{-1}, which is 5% higher than the value of 5 μ_B FU^{-1} as expected based on the Slater–Pauling rule which is equal to $(18 + 8 + 3) - 24 = 5$ μ_B FU^{-1}. Analogous to the results as obtained in Co_2FeAl it becomes important to study the variation of magnetic moment in terms of effective magnetic hyperfine fields as deduced using Mössbauer spectroscopy with respect to valence as deduced theoretically based on Slater–Pauling rule. As a first step the variation of mean hyperfine fields corresponding to different Co_2YZ with the effective electron valence of each compound is deduced. Shown are the Mössbauer spectra (*cf.* Fig. 4) deduced in the Cr doped compounds of interest such as $Co_2Fe_{0.8}Cr_{0.2}Al$ and $Co_2Fe_{0.5}Cr_{0.5}Al$ along with those obtained in $Co_2FeAl_{0.5}Si_{0.5}$, Co_2FeAl, $Co_2FeAl_{0.95}$. These compounds are so chosen such that B_2 type of disordering get affected by different means such as substitution at Y/Z sites causing valence/size difference affecting magnetic interactions between the atoms. Also it is important to note that the spin polarization coefficient is reported to be of the order of 80% and 60% in the case of $Co_2FeAl_{0.5}Si_{0.5}$ and Co_2FeAl respectively. The values of the hyperfine parameters as deduced in these systems are shown in Table 2. In these fitting, the line width of the different components is kept fixed as 0.28 mm s^{-1}. The error in the relative fractions remains well with in 0.01. Spectra are best fitted in all the cases with the value of Chi square ranging 1.05 ± 0.22.

The variation of the mean hyperfine fields deduced at Fe sites in different Co based Heusler compounds as mentioned above with respect to electron valence is shown in the Fig. 5. It is important to see that the value of the hyperfine field is the maximum in the compound $Co_2FeAl_{0.5}Si_{0.5}$ which is reported to exhibit a high value of spin polarization thereby establishing the consistency of the Mössbauer results with the spintronic properties of these materials. Interestingly the Mössbauer results elucidate a close correlation between the lattice ordering with the spin polarization. The value of the mean hyperfine field is seen to be smaller in Co_2FeAl. In the case of Al deficient compound it is observed to decrease further indicating the effect of Al vacancies on the magnetization which is deduced based on the mean value of the hyperfine field at the Fe sites.[23] The values of the mean hyperfine fields corresponding to Cr doped Co_2FeAl are seen to be decreasing with increasing Cr composition as shown in the Fig. 5.

Results on the effect of quenching on the disordering as obtained in $Co_2Fe_{0.8}Cr_{0.2}Al$ in the present study is compared with that of Co_2FeAl subjected to similar non-equilibrium defects. The respective Mössbauer spectra are shown in Fig. 6. In the case of $Co_2Fe_{0.8}Cr_{0.2}Al$, it can be seen (*cf.* Table 2) that the fractions of Fe atoms, close to 15%, are associated with typical values close to 25 tesla and lesser along with non-magnetic fractions experiencing 0 tesla. These fractions are interpreted to be due to Fe atoms associated with A_2 type of disordering of different varying degree. It is further seen that the defects associated fractions in the case of the as melted $Co_2Fe_{0.5}Cr_{0.5}Al$ increases close to 30% (*cf.* Table 2). Based on the variation of the values of the mean hyperfine field of different Co based Heusler compounds as shown in Fig. 5, it can be inferred that there is a change of slope in the Cr substituted compounds and in particular the values of the mean hyperfine fields are seen to decrease in the case of the compound with equal substitution of Cr at Fe sites which may be indication of an enhanced lattice disordering.

Importantly the Cr substitution is interpreted to have been significantly affecting the magnetic properties of the matrix containing Fe and Co atoms having appreciable values of magnetic moments. In order to get a good understanding of the lattice disorder with a clear delineation of the effects due to Cr doping, in particular while subjected to non-equilibrium treatments it is important to compare the results as obtained in the pristine Co_2FeAl in which defects are introduced in a similar manner. In this study the effects of lattice disorder due to quenching treatments have been studied in Cr doped Co_2FeAl and compared with that of the results of the pristine Co_2FeAl subjected to similar quenching studies which is discussed as follows.

Mössbauer (MS) results as obtained in the $Co_2Fe_{0.8}Cr_{0.2}Al$ subjected to quenching and annealing treatments are compared with that of Co_2FeAl subjected to quenching in the

Table 3 Hyperfine parameters as obtained in $Co_2Fe_{0.5}Cr_{0.5}Al$ subjected to different heat treatment conditions as explained involving quenching and isochronal annealing carried out at different temperatures

Sample treatment	(i)	δ_i (mm s^{-1})	Δ_i (mm s^{-1})	B_{hf} (T)	f_i
As melted $Co_2Fe_{0.5}Cr_{0.5}Al$ (a)	1	−0.07 ± 0.01	−0.03 ± 0.02	30.35 ± 0.11	0.27
	2	0.11 ± 0.02	0.05 ± 0.02	26.83 ± 0.15	0.16
	3	0.38 ± 0.04	0.28 ± 0.08	21.09 ± 0.28	0.12
	4	0.24 ± 0.02	0.34 ± 0.03	0	0.09
	5	0.06 ± 0.01	0.05 ± 0.02	28.70 ± 0.11	0.30
	6	0.12 ± 0.04	0.18 ± 0.08	7.45 ± 0.25	0.07
$Co_2Fe_{0.5}Cr_{0.5}Al$-1073 K-2 h-quenched (b)	1	−0.02 ± 0.001	−0.08 ± 0.04	28.88 ± 0.09	0.35
	2	0.08 ± 0.04	0.25 ± 0.08	28.94 ± 0.21	0.13
	3	0.04 ± 0.02	0.08 ± 0.03	26.13 ± 0.20	0.13
	4	0.15 ± 0.03	−0.11 ± 0.07	13.12 ± 0.25	0.08
	5	−0.04 ± 0.01	0	0	0.31
$Co_2Fe_{0.5}Cr_{0.5}Al$-1273 K-2 h-quenched (c)	1	0.05 ± 0.02	0.10 ± 0.04	30.812 ± 0.16	0.17
	2	0.04 ± 0.01	0.06 ± 0.02	28.84 ± 0.10	0.3
	3	−0.05 ± 0.01	0	0	0.37
	4	0.27 ± 0.05	0.49 ± 0.09	22.81 ± 0.31	0.06
	5	0.16 ± 0.06	0.08 ± 0.03	15.93 ± 0.36	0.06
	6	0.40 ± 0.06	0.59 ± 0.10	0	0.04
$Co_2Fe_{0.5}Cr_{0.5}Al$, quenching temp (T_q) T_q = 1073 K; annealing temp (T_a) T_a = 573 K 2 h (d)	1	0.02 ± 0.01	0.05 ± 0.01	30.3 ± 0.12	0.25
	2	0.03 ± 0.01	0.06 ± 0.02	28.5 ± 0.56	0.32
	3	0.07 ± 0.02	0.14 ± 0.01	26.1 ± 0.82	0.2
	4	−0.10 ± 0.02	0.4 ± 0.1	0	0.13
	5	−0.12 ± 0.01	0	0	0.10
$Co_2Fe_{0.5}Cr_{0.5}Al$, quenching temp (T_q) T_q = 1073 K; annealing temp (T_a) T_a = 573 K/673 K/723 K (e)	1	0.03 ± 0.01	−0.04 ± 0.01	31.69 ± 0.17	0.12
	2	−0.02 ± 0.065	−0.11 ± 0.03	29.56 ± 0.05	0.3
	3	0.05 ± 0.01	0.21 ± 0.06	29.51 ± 0.11	0.15
	4	0.04 ± 0.011	−0.04 ± 0.01	27.40 ± 0.08	0.17
	5	0.19 ± 0.04	0	0	0.04
	6	−0.1 ± 0.02	0.16 ± 0.03	0	0.15
	7	0.5 ± 0.05	0.52 ± 0.07	14.02 ± 0.4	0.07
$Co_2Fe_{0.5}Cr_{0.5}Al$, quenching temp (T_q) T_q = 1073 K; annealing temp (T_a) T_a = 573 K/ 673 K/723 K/773 K (f)	1	0.04 ± 0.02	0.09 ± 0.03	31.05 ± 0.34	0.15
	2	0.04 ± 0.02	−0.02 ± 0.01	29.95 ± 0.23	0.27
	3	−0.06 ± 0.01	0	0	0.19
	4	0.04 ± 0.01	0.2 ± 0.07	26.54 ± 0.23	0.07
	5	0.05 ± 0.01	0.04 ± 0.02	26.57 ± 0.10	0.32
$Co_2Fe_{0.5}Cr_{0.5}Al$-mag, 0.3 T magnetic field	1	0.04 ± 0.01	0.05 ± 0.03	30.87 ± 0.10	0.24
	2	0.04 ± 0.01	0.07 ± 0.01	29.24 ± 0.06	0.41
	3	0.13 ± 0.02	−0.01 ± 0.03	26.97 ± 0.14	0.18
	4	0.33 ± 0.06	0.42 ± 0.10	10.94 ± 0.40	0.08
	5	0.36 ± 0.02	0.45 ± 0.04	0	0.09
$Co_2Fe_{0.5}Cr_{0.5}Al$-melted 673 K annealing (g)	1	−0.04 ± 0.01	0.02 ± 0.01	30.8 ± 0.05	0.37
	2	−0.03 ± 0.01	−0.02 ± 0.01	29.35 ± 0.06	0.41
	3	−0.02 ± 0.01	−0.08 ± 0.04	27.36 ± 0.21	0.09
	4	0.02 ± 0.01	0.311 ± 0.04	0	0.05
	5	0.31 ± 0.03	−0.76 ± 0.05	16.94 ± 0.25	0.08

Fig. 6. The values of the hyperfine parameters are shown in the Table 2. It can be seen that in Co_2FeAl subjected to quenching, there is an increase in the value of non-magnetic fraction accompanied by about 5% of the Fe atoms experiencing hyperfine fields much lower than that of the defect free sites. This implies that these are due to Fe atoms associated with A_2 type of disordering as has been reported.[31–44] Based on the comparison of the MS results as obtained in the as melted and quenched $Co_2Fe_{0.8}Cr_{0.2}Al$ it could be deduced that there are no appreciable changes in the hyperfine parameters associated with Fe atoms subsequent to quenching treatment. This might imply that the Co_2FeAl substituted with 20% of Cr atoms remains almost robust against an increase in the lattice disordering due to quenching effects. Having studied the effect of Cr addition on the lattice disordering based on the studies carried out so far, the following part of the manuscript is mainly

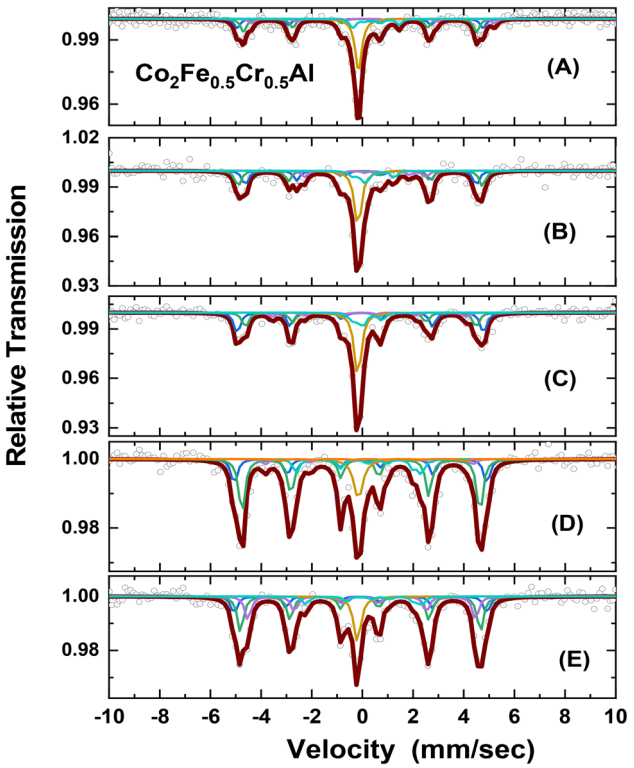

Fig. 9 Mössbauer spectra as obtained in $Co_2Fe_{0.5}Cr_{0.5}Al$ at 300 K subsequent to subjecting the samples to different treatments *viz.*, heat treatment at 1073 K for 2 h and furnace cooled (FC) to room temperature followed by (A) annealing at 623 K for 6 h and quenched (B) annealing at 673 K for 6 h and quenched (C) sample (B) with the application of external magnetic field of 0.3 tesla. Heat treatment at 1073 K for 2 h and quenched to room temperature followed by (D) annealing at 773 K for 2 h and furnace cooled (FC) and (E) annealing at 873 K for 2 h and furnace cooled (FC).

focussed towards understanding the formation and annealing of defects in $Co_2Fe_{0.5}Cr_{0.5}Al$ subjected to quenching.

Mössbauer spectra as obtained in $Co_2Fe_{0.5}Cr_{0.5}Al$ subjected to different quenching & annealing treatments are shown in Fig. 7. In the case of as melted $Co_2Fe_{0.5}Cr_{0.5}Al$ close to 30% of Fe atoms are observed to be experiencing values of hyperfine fields much lesser than that corresponding to ordered sites experiencing values of hyperfine fields close to 28 tesla as can be seen in the Table 2. The fraction of Fe atoms experiencing non-magnetic interactions accompanied by lattice distortion as revealed by the high value of quadrupole splitting is also seen to have increased to 10% in the case of $Co_2Fe_{0.5}Cr_{0.5}Al$ while this fraction remained as 5% in the case of $Co_2Fe_{0.8}Cr_{0.2}Al$. Fe atoms associated with defects associated sites experience lower values of hyperfine fields with increasing degree of A_2 type of disorder in the case of both 20% and 50% Cr doped Co_2FeAl as can be seen in the Table 2. In contrast to MS results as obtained in the quenched $Co_2Fe_{0.8}Cr_{0.2}Al$ as discussed earlier, the defects associated fractions are seen to increase to about 50% as deduced based on the Mössbauer studies carried out in $Co_2Fe_{0.5}Cr_{0.5}Al$ following quenching from 1073 K. The decrease in hyperfine fields in Cr substituted Co_2FeAl is mainly understood due to increase in the defects induced disordered sites leading to reduction in the magnetic moments at Fe sites. There is an antiferromagnetic coupling exists between Cr atoms occupying antisites with the atoms of Co/Cr occupying regular ordered sites. Importantly such a negative contribution to total magnetic moment is understood to result in the reduced values of the hyperfine fields at Fe sites (as shown in Fig. 8) associated with such disordered sites.

As high as 30% of Fe atoms are exposed to cubic and non-magnetic sites having zero values of quadrupole shift and hyperfine fields in the case of quenched $Co_2Fe_{0.5}Cr_{0.5}Al$ which is absent in the case of $Co_2Fe_{0.8}Cr_{0.2}Al$. One lot of the $Co_2Fe_{0.5}Cr_{0.5}Al$ sample was quenched from 1073 K and was subjected to isochronal annealing treatment at different temperature for a time interval of 2 h and after each annealing step the Mössbauer studies were carried out at 300 K.

Based on the comparison of the results as obtained in pristine and Cr substituted Co_2FeAl subjected to quenching it is observed that the defects and hence the lattice disordering effects are significant particularly in $Co_2Fe_{0.5}Cr_{0.5}Al$ while such effects are less in Co_2FeAl. This brings out the importance of Cr–Co and Fe–Co related type of antisite defects leading to appreciable increase in A_2 type of disordering. Mössbauer studies carried out at 300 K in the as quenched $Co_2Fe_{0.5}Cr_{0.5}Al$ shows that these types of defects associated fractions of Fe atoms is increased up to 50%. From the Table 3 it can be seen that in the quenched sample the fractions of Fe atoms associated with cubic sites experiencing non-magnetic interactions has got increased by 20% as compared to that of the melted $Co_2Fe_{0.5}Cr_{0.5}Al$. Non-magnetic fraction is seen to increase to 40% in the case of another lot of $Co_2Fe_{0.5}Cr_{0.5}Al$ sample quenched from 1273 K. The results of the isochronal annealing studies on the sample quenched from 1073 K are discussed as follows.

Results of the Mössbauer studies carried out following the annealing of the quenched sample at 573 K show that the fraction of non-magnetic sites characterizing A_2 type of defects induced disordering decreased by 0.07 (*cf.* Table 3). Commensurately the values of hyperfine fields associated with ordered sites are seen to exhibit an increase. This implies that an appreciable increase in the lattice ordering is seen right from annealing at 573 K. Annealing at 673 K shows an appreciable recovery of defects leading to an increase in the fractions associated with ordered sites. Following annealing at 723 K the defects associated fraction remains almost same as that of the one corresponding to the as melted sample. Isochronal annealing results are shown (Fig. 8) in terms of the variation of $\langle B_{hf} \rangle$ and the ordered fraction with the isochronal annealing temperature. These results show that in the as quenched sample the fractions of Fe atoms associated with disordered sites increase commensurately resulting in a low value of the mean hyperfine field $\langle B_{hf} \rangle$. With increasing annealing temperature the ordered fractions and the value of the effective magnetic hyperfine fields are observed to increase and attain maximum value following annealing in the interval 673 K. Annealing beyond this temperature is observed to result in a slight decrease in these values. Therefore based on the results of the present study it could be deduced that the maximum

Table 4 Results of Mössbauer parameters as obtained in $Co_2Fe_{0.5}Cr_{0.5}Al$ subjected to two steps of heat treatments involving quenching (Q) and/or furnace cooling (FC)

Sample treatment	(i)	δ_i (mm s^{-1})	Δ_i (mm s^{-1})	B_{hf} (T)	f_i
$Co_2Fe_{0.5}Cr_{0.5}Al$-1073 K 2 h-FC-623 K 6 h-Q (A)	1	0.02 ± 0.02	0.01 ± 0.03	30.11 ± 0.15	0.19
	2	0.03 ± 0.01	−0.01 ± 0.02	28.54 ± 0.10	0.27
	3	0.41 ± 0.04	0.25 ± 0.07	29.75 ± 0.24	0.09
	4	−0.04 ± 0.01	0	0	0.34
	5	0.49 ± 0.03	0.30 ± 0.07	5.77 ± 0.20	0.11
$Co_2Fe_{0.5}Cr_{0.5}Al$-1073 K 2 h-FC-673 K 6 h-Q (B)	1	0.11 ± 0.02	−0.11 ± 0.04	28.27 ± 0.40	0.24
	2	0.01 ± 0.02	−0.05 ± 0.03	29.91 ± 0.12	0.25
	3	0.41 ± 0.05	−0.37 ± 0.10	14.84 ± 0.37	0.1
	4	−0.05 ± 0.01	0	—	0.3
	5	0.40 ± 0.05	0.77 ± 0.16	3.58 ± 0.49	0.11
$Co_2Fe_{0.5}Cr_{0.5}Al$-1073 K 2 h-FC-673 K 6 h-Q-mag (C)	1	0.06 ± 0.01	−0.04 ± 0.02	30.13 ± 0.08	0.3
	2	0.03 ± 0.02	0.06 ± 0.03	28.24 ± 0.11	0.22
	3	0.22 ± 0.06	0.32 ± 0.12	23.70 ± 0.35	0.06
	4	0.30 ± 0.01	0	0	0.3
	5	0.21 ± 0.04	0.66 ± 0.10	2.17 ± 0.32	0.12
$Co_2Fe_{0.5}Cr_{0.5}Al$-1073 K 2 h-Q-773 K 2 h-FC (D)	1	0.03 ± 0.01	0.01 ± 0.02	30.9 ± 0.09	0.2
	2	0.04 ± 0.01	0.04 ± 0.01	29.13 ± 0.04	0.44
	3	0.39 ± 0.06	−0.05 ± 0.02	25.4 ± 0.42	0.05
	4	−0.04 ± 0.01	0	0	0.18
	5	0.38 ± 0.02	−0.72 ± 0.05	15.35 ± 0.18	0.1
	6	0.41 ± 0.18	0.24 ± 0.01	22.6 ± 1.20	0.03
$Co_2Fe_{0.5}Cr_{0.5}Al$-1073 K 2 h-Q-773 K 2 h-FC-873 K 2 h-FC (E)	1	0.02 ± 0.01	0.05 ± 0.03	30.9 ± 0.12	0.17
	2	0.02 ± 0.01	0.036 ± 0.02	29.35 ± 0.08	0.35
	3	0.06 ± 0.01	0.059 ± 0.02	27.84 ± 0.10	0.23
	4	−0.09 ± 0.001	0	0	0.16
	5	0.45 ± 0.04	−0.67 ± 0.06	13.75 ± 0.27	0.09

recovery of A_2 type of defects occurs following annealing treatments at 673 K in $Co_2Fe_{0.5}Cr_{0.5}Al$ subjected to quenching at 1073 K. Thus the effect of the recovery of defects has been addressed in $Co_2Fe_{0.5}Cr_{0.5}Al$ quenched from elevated temperature of 1073 K followed by isochronal annealing studies. To understand the effect of quenching rate on the subsequent recovery of defects in the following the role of defects ordering/disordering will be discussed in the system subsequent to furnace cooling after annealing of the sample $Co_2Fe_{0.5}Cr_{0.5}Al$ at 1073 K for 2 h.

Mössbauer studies (MS) are carried out in the sample furnace cooled from 1073 K. Mössbauer spectra as obtained at room temperature in the furnace cooled samples subsequent to different annealing treatments are given in the Fig. 9 and the deduced hyperfine parameters are listed in the Table 4. These results show that the values of the hyperfine fields associated with ordered Fe sites are seen to be smaller as compared to that of the sample quenched from 1073 K. It is observed that the values of hyperfine fields corresponding to disordered sites which are rich in A_2 type of disordered zones are smaller. In addition the fraction of Fe atoms associated with zero hyperfine fields which are understood to be due to Cr rich caused due to appreciably high A_2 type of disordering. This is understood due to Fe atoms associated with enriched Cr → Co antisites. The mean hyperfine field corresponding to sample subjected to annealing at 1073 K for 2 h followed by furnace cooling is observed to be much smaller as compared to sample annealed at 1073 K for 2 h and quenched. In the case of the sample annealed at 1073 K for 2 h and furnace cooled (FC) while annealed at 673 K for a duration of 6 h there is a decrease in the mean hyperfine in contrast to that observed in the case of the sample annealed at 1073 K for 2 h and quenched followed by annealing at 673 K. Comparison of MS results imply that the defects structures in both the cases of sample quenched/furnace cooled from 1073 K are basically same with A_2 type of the fractions of Fe atoms associated with disordered zones in the case of FC samples are much higher. There is no appreciable decrease in the defects associated fractions following annealing studies on the FC sample. Based on these results it is interpreted that the in the FC sample the disordered zones formed might be of much larger size as compared to that of the sample quenched from 1073 K. Hence in spite of annealing of the furnace cooled sample at 673 K no appreciable recovery of defects has been observed. Therefore, annealing at low temperatures close to 673 K in the case of Co_2FeAl quenched from 1073 K lead to a significant recovery of A_2 type of defects becoming almost close to that of the as melted sample. On the other hand 1073 K quenched sample even if subjected to annealing at temperatures 773 K and 873 K and furnace cooled there is an appreciable recovery of defects similar as that of 1073 K quenched sample subjected to annealing at 673 K and quenched. Hence this study implies that A_2 type of disordering could be reduced in the sample due to annealing treatments in the quenched sample where as in FC cooled sample such a recovery of defects could not be achieved as understood due to the formation of coarse A_2 type of disordered zones in the later which remain quite stable against recovery due to annealing treatments. As we have see that there is no recovery of defects in

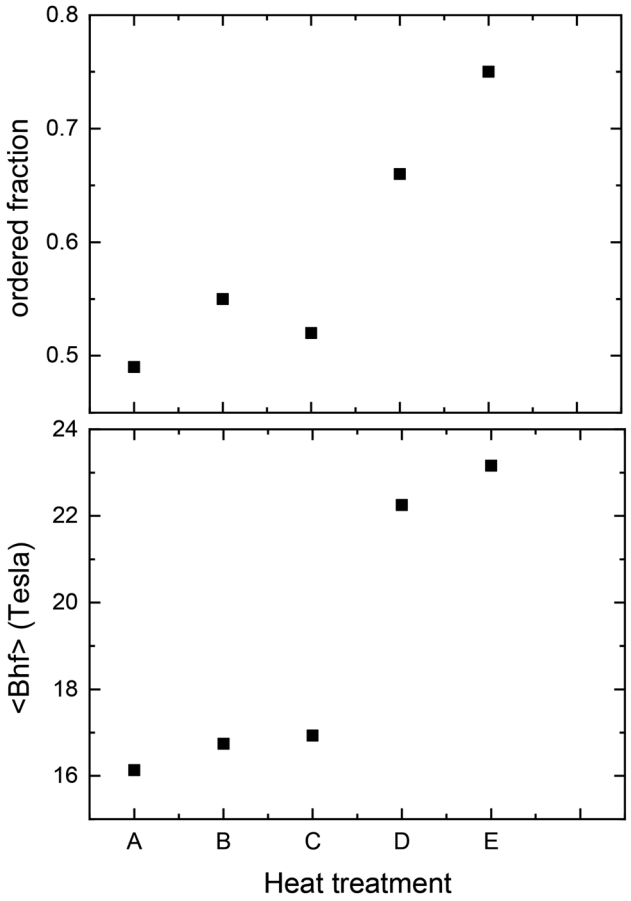

Fig. 10 Variation of the magnitude of the ordered fractions is observed to be correlated with the value of the mean hyperfine field in the case of $Co_2Fe_{0.5}Cr_{0.5}Al$ subjected to two steps of annealing involved quenching (Q) and/or furnace cooling (FC). Here (A) 1073 K 2 h-FC-623 K 6 h-Q (B) 1073 K-2 h-FC-673 K 6 h-Q (C) 1073 K 2 h-FC-673 K-6 h-Q-mag (D) 1073 K 2 h-Q-773 K 2 h-FC and (E) 1073 K 2 h-Q-773 K 2 h-FC-873 K 2 h-FC.

1073 K FC and 673 K quenched sample as seen in the quenched sample interpreted to be due to the formation of A_2 type of disordered zones which are much larger in the matrix these samples are subjected to mechanical milling for 3 h to see if there are any changes in the hyperfine parameters as experienced by Fe atoms leading to enhanced ordering. An enhanced ordered fractions and hence the mean hyperfine field has been observed in the 1073 K FC + 673 K 6 h quenched sample following mechanical milling. It is observed that subsequent to a moderate milling there is a reduction in the fraction of Fe atoms associated with Cr rich zones leading to the presence of Fe sites experiencing magnetic hyperfine fields which are larger in values as compared to that of the quenched sample. This result could be explored to further reduce Cr rich zones by means of repeated cold working/milling followed by annealing at 673 K. Results of these studies on quenched sample subjected to annealing at 1073 K and either quenched or furnace cooled to 300 K in terms of the variation of the mean value of the hyperfine field $\langle B_{hf} \rangle$ and ordered fractions with concerned treatment are shown in Fig. 10. This study implies that these Cr rich zones might be occurring at grain boundaries as evidenced by the decrease in the disordered fractions followed by milling. Occurrence of Cr rich zones in Heusler compounds was confirmed based on TEM results.[37,38]

It is already observed that about 0.6 fraction of Fe atoms are seen to be associated with ordered sites, while the remaining 0.4 fractions of Fe atoms are occupying disordered sites mainly of A_2 type in $Co_2Fe_{0.5}Cr_{0.5}Al$ melted sample. Based on the results as obtained in the present study the as melted sample is subjected to annealing at 673 K for 2 h to look for the recovery of defects. Mössbauer spectra obtained in as melted $Co_2Fe_{0.5}Cr_{0.5}Al$ and subsequent to annealing at 673 K for 2 h are shown in Fig. 11 and the results of hyperfine parameters are shown in the Table 5. It is striking to see that the fractions associated with disordered sites decrease from 0.4 to close to 0.2, which is a significant result of the present study. It is understood that in the as melted sample small zones of A_2 disordered sites get formed. These get dissociated appreciably following the annealing at 673 K leading to a significant increase in the fraction of Fe atoms associated with ordered sites. Interesting results of this study in terms of enhanced lattice ordering leading to appreciable increase in the magnetic ordering deduced based on the values of the mean hyperfine magnetic fields are comprehended as follows.

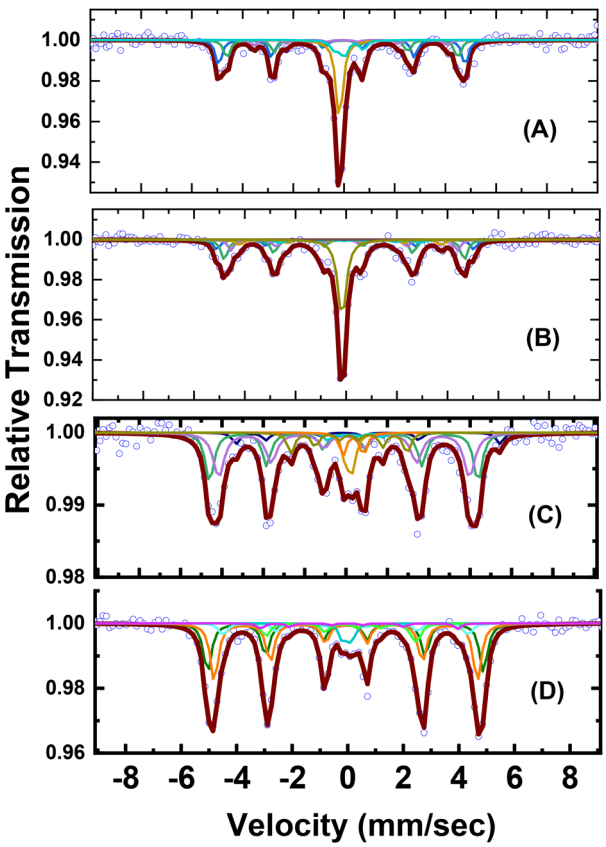

Fig. 11 Mössbauer spectra corresponding to $Co_2Fe_{0.5}Cr_{0.5}Al$ subjected to (A) 1073 K 2 h-FC and 673 K 6 h quenched under $B_{ext} = 0.3$ T, (B) sample (A) after milling for 3 h under $B_{ext} = 0.3$ T, (C) as melted $Co_2Fe_{0.5}Cr_{0.5}Al$, (D) melted sample after annealing at 673 K under $B_{ext} = 0.3$ T

Table 5 Hyperfine parameters as obtained in $Co_2Fe_{0.5}Cr_{0.5}Al$, subjected to different treatments involving furnace cooling (FC)/mechanically milling, based on the Mössbauer studies carried out at 300 K and under the application of magnetic field

Sample treatment	(i)	δ_i (mm s^{-1})	Δ_i (mm s^{-1})	B_{hf} (T)	f_i
$Co_2Fe_{0.5}Cr_{0.5}Al$-1073 K 2 h-FC-673 K 6 h-Q-mag (A)	1	0.18 ± 0.01	−0.04 ± 0.02	30.13 ± 0.08	0.3
	2	0.03 ± 0.02	0.06 ± 0.03	28.24 ± 0.10	0.22
	3	0.22 ± 0.06	0.32 ± 0.11	23.7 ± 0.35	0.06
	4	0.30 ± 0.01	0	0	0.3
	5	0.21 ± 0.04	0.66 ± 0.10	2.17 ± 0.33	0.12
$Co_2Fe_{0.5}Cr_{0.5}Al$-1073 K 2 h-FC-673 K 6 h-Q-3 h-milled-mag (B)	1	0.24 ± 0.03	0.17 ± 0.05	31.40 ± 0.19	0.12
	2	0.03 ± 0.01	0.04 ± 0.03	29.36 ± 0.10	0.25
	3	−0.02 ± 0.02	0.12 ± 0.05	27.73 ± 0.24	0.12
	4	−0.01 ± 0.04	−0.19 ± 0.09	24.71 ± 0.29	0.07
	5	0.38 ± 0.07	−0.22 ± 0.13	17.15 ± 0.46	0.07
	6	−0.05 ± 0.04	0	0	0.37
As melted-$Co_2Fe_{0.5}Cr_{0.5}Al$ (C)	1	−0.07 ± 0.01	−0.03 ± 0.02	30.35 ± 0.11	0.27
	2	0.11 ± 0.02	0.05 ± 0.02	26.83 ± 0.15	0.16
	3	0.38 ± 0.04	0.28 ± 0.08	21.09 ± 0.28	0.12
	4	0.24 ± 0.02	0.34 ± 0.03	0	0.09
	5	0.06 ± 0.01	0.05 ± 0.02	28.70 ± 0.11	0.3
	6	0.12 ± 0.04	0.18 ± 0.08	7.45 ± 0.25	0.07
$Co_2Fe_{0.5}Cr_{0.5}Al$-melted-673 K 6 h-mag (D)	1	−0.04 ± 0.01	0.02 ± 0.01	30.8 ± 0.05	0.34
	2	−0.03 ± 0.01	−0.02 ± 0.01	29.35 ± 0.06	0.41
	3	−0.02 ± 0.01	−0.08 ± 0.04	27.36 ± 0.21	0.09
	4	0.02 ± 0.01	0.311 ± 0.04	0	0.05
	5	0.31 ± 0.03	−0.76 ± 0.05	16.94 ± 0.25	0.08
	6	0.22 ± 0.06	0.45 ± 0.13	22.06 ± 0.43	0.03

Due to enhanced A_2 type of disordering fine Cr rich zones are primarily formed at the grain boundaries in the ferromagnetic matrix. Magnetic ordering temperature for Cr rich Fe–Cr has been reported to be close to 673 K.[38–40] Hence annealing at a temperature close to 673 K is expected to result in reduction of Fe–Cr repulsion mediated by spin frustration due to AFM interaction between Fe and Cr atoms. This is understood to result in the enhancement of magnetically ordered zones with the partial dissolution of Cr rich zones. As these zones are occurring nearby grain boundaries moderate annealing at 673 K which is importantly coinciding with the magnetic ordering temperature of the Cr rich Fe–Cr zones an appreciable dissolution of these zones is observed.

Based on the results of this study the as melted $Co_2Fe_{0.5}Cr_{0.5}Al$ sample from one lot has been subjected to annealing at 673 K for 6 h and quenched to study the recovery of A_2 type of defects present in the as melted sample. Strikingly about 20% of recovery of defects is observed after the above annealing treatment. Hence based on the results of this study, it is suggested that by keeping the substrate temperature at 673 K it might be possible to prepare Heusler compounds based thin films of $Co_2Fe_{0.5}Cr_{0.5}Al$/$Co_2Fe_{0.8}Cr_{0.2}Al$ with reduced defect concentration having ordered lattice. Therefore the results of the present study might have significant implications on the application of these samples either the bulk or thin film by means of reducing the A_2 type of disordered zones due to proper annealing treatments as suggested in this study.

Summarizing, this work reports the effects of ordering/disordering of the lattice due to magnetic interactions between Fe,Co and Cr atoms in $Co_2Fe_{1-x}Cr_xAl$, particularly addressed in a detailed manner in $Co_2Fe_{0.5}Cr_{0.5}Al$, as compared with that of pristine Co_2FeAl and $Co_2FeAl_{0.5}Si_{0.5}$. Further the effect of non-equilibrium treatments on the Cr substituted samples *viz.,* $Co_2Fe_{0.8}Cr_{0.2}Al$ and $Co_2Fe_{0.5}Cr_{0.5}Al$ has been addressed extensively. The partial presence of Co–Cr and Co–Fe type of antisite defects leading to A_2 type of disordered lattice of the as melted $Co_2Fe_{0.8}Cr_{0.2}Al$ has been observed along with the dominantly present ordered sites. Significant increase in the fractions of Fe atoms associated with the A_2 type of disordering is observed in $Co_2Fe_{0.5}Cr_{0.5}Al$ subjected to quenching which is elucidated in this study. Having observed the appreciable influence of the quenching effects on the lattice disordering in $Co_2Fe_{0.5}Cr_{0.5}Al$, controlled annealing studies have been carried out to address the defect recovery which show the appreciable recovery of lattice ordering following annealing treatment at 673 K. Based on the results as deduced in this study the as melted $Co_2Fe_{0.5}Cr_{0.5}Al$ has been subjected to annealing at 673 K for 6 h which has resulted in a defect recovery by close to 20% leading to an appreciable increase in the lattice ordering. In the annealed system, the disordered fraction has got reduced to as low as 5% which is a striking result of the present study which could be of immense potential with respect to applications of Cr substituted Co_2FeAl based systems including bulk and thin films based hetero structures for spintronic applications.

4. Conclusion

The partial presence of Co–Cr and Co–Fe type of antisite defects leading to A_2 disordered lattice of the as melted $Co_2Fe_{0.8}Cr_{0.2}Al$ has been observed along with the dominantly present ordered sites. Significant increase in defects associated fractions, in particular of A_2 type of defects, is observed in the case of

$Co_2Fe_{0.5}Cr_{0.5}Al$ subjected to quenching. This is understood to result in an enhanced lattice disorder leading to a sharp reduction in the mean value of the magnetic hyperfine fields as deduced at Fe sites. Isochronal annealing studies on the quenched $Co_2Fe_{0.5}Cr_{0.5}Al$ show that the optimal recovery of defects occurs following annealing at 673 K. This experimental finding might have significant impact on the utilization of Cr substituted Co_2FeAl systems for highly efficient spintronic devices. This study therefore elucidates an important role of the manifestation of the magnetic interactions especially between Fe, Co and Cr atoms leading to significant changes in the concentration and specific types of defects selectively produced in $Co_2Fe_{0.5}Cr_{0.5}Al$ as compared with that of $Co_2Fe_{0.8}Cr_{0.2}Al$ subjected to similar non-equilibrium treatments in this study. The effective value of the hyperfine field is also observed to be correlated with the degree of ordering/disordering of the lattice with the Fe atoms associated with ordered sites experiencing much higher value of the hyperfine field as compared to that of the disordered sites. This study also proposes optimal annealing treatment for the recovery of defects in $Co_2Fe_{0.5}Cr_{0.5}Al$, which would be of significant importance in these spintronic materials.

Conflicts of interest

There are no conflicts to declare.

References

1 S. A. Wolf, D. D. Awschalom, R. A. Buhrman, J. M. Daughton, S. Molnar von, M. L. Roukes, A. Y. Chtchelkanova and D. M. Treger, *Science*, 2001, **294**, 1488–1495.
2 R. A. de Groot, F. M. Meuller, P. G. Van Engen and K. J. Buschow, *Phys. Rev. Lett.*, 1983, **50**, 2024.
3 X. L. Wang, *Phys. Rev. Lett.*, 2008, **100**, 1–4.
4 I. Galanakis, K. Özdoğan, E. Şaşıoğlu, I. Galanakis, K. Özdoğan and E. Şaşıoğlu, *AIP Adv.*, 2016, **6**, 1–6.
5 V. Alijani, S. Ouardi, G. H. Fecher, J. Winterlik, S. S. Naghavi, X. Kozina, G. Stryganyuk, C. Felser, E. Ikenaga, Y. Yamashita, S. Ueda and K. Kobayashi, *Phys. Rev. B: Condens. Matter Mater. Phys.*, 2011, **84**, 1–10.
6 G. H. Fecher, H. C. Kandpal, S. Wurmehl, C. Felser and G. Schönhense, *J. Appl. Phys.*, 2006, **99**, 2–5.
7 J. E. Fischer, J. Karel, S. Fabbrici, P. Adler, S. Ouardi, G. H. Fecher, F. Albertini and C. Felser, *Phys. Rev. B*, 2016, **94**, 1–8.
8 M. Vahidi, J. A. Gifford, S. K. Zhang, S. Krishnamurthy, Z. G. Yu, L. Yu, M. Huang, C. Youngbull, T. Y. Chen and N. Newman, Fabrication of highly spin-polarized Co2FeAl 0.5Si0.5 thin-films, *APL Mater.*, 2014, **2**, 7.
9 T. Ishikawa, S. Hakamata, K. Matsuda, T. Uemura and M. Yamamoto, *J. Appl. Phys.*, 2008, **103**, 07A919.
10 L. Bainsla, A. I. Mallick, A. A. Coelho, A. K. Nigam, B. S. D. C. S. Varaprasad, Y. K. Takahashi, A. Alam, K. G. Suresh and K. Hono, *J. Magn. Magn. Mater.*, 2015, **394**, 82–86.
11 J. S. Moodera and G. Mathon, *J. Magn. Magn. Mater.*, 1999, **200**, 248–273.
12 N. Auth, G. Jakob, T. Block and C. Felser, *Phys. Rev. B: Condens. Matter Mater. Phys.*, 2003, **68**, 1–6.
13 Y. Sakuraba, M. Hattori, M. Oogane, Y. Ando, H. Kato, A. Sakuma, T. Miyazaki and H. Kubota, *Appl. Phys. Lett.*, 2006, **88**, 192508.
14 N. Tezuka, N. Ikeda, S. Sugimoto and K. Inomata, *Appl. Phys. Lett.*, 2006, **89**, 10–13.
15 R. J. Soulen, J. M. Byers, M. S. Osofsky, B. Nadgorny, T. Ambrose, S. F. Cheng, P. R. Broussard, C. T. Tanaka, J. Nowak, J. S. Moodera, A. Barry and J. M. D. Coey, *Science*, 1998, **282**, 85–88.
16 L. Makinistian, M. M. Faiz, R. P. Panguluri, B. Balke, S. Wurmehl, C. Felser, E. A. Albanesi, A. G. Petukhov and B. Nadgorny, *Phys. Rev. B: Condens. Matter Mater. Phys.*, 2013, **87**, 1–5.
17 K. Inomata, M. Wojcik, E. Jedryka, N. Ikeda and N. Tezuka, *Phys. Rev. B: Condens. Matter Mater. Phys.*, 2008, **77**, 1–2.
18 J. Karel, J. E. Fischer, S. Fabbrici, E. Pippel, P. Werner, M. Vinicius Castergnaro, P. Adler, S. Ouardi, B. Balke, G. H. Fecher, J. Morais, F. Albertini, S. S. P. Parkin and C. Felser, *J. Mater. Chem. C*, 2017, **5**, 4388–4392.
19 B. Ravel, J. O. Cross, M. P. Raphael, V. G. Harris, R. Ramesh and L. V. Saraf, *Appl. Phys. Lett.*, 2002, **81**, 2812–2814.
20 F. Li, B. Yang, J. Zhang, X. Han and Y. Yan, *Phys. Chem. Chem. Phys.*, 2020, **22**, 716–723.
21 X. Zhang, H. Xu, B. Lai, Q. Lu, X. Lu, Y. Chen, W. Niu, C. Gu, W. Liu, X. Wang, C. Liu, Y. Nie, L. He and Y. Xu, *Sci. Rep.*, 2018, **8**, 5–10.
22 M. Zhang, Z. Liu, H. Hu, G. Liu, Y. Cui, J. Chen, G. Wu, X. Zhang and G. Xiao, *J. Magn. Magn. Mater.*, 2004, **277**, 130–135.
23 R. K. Yadav and R. Govindaraj, *Phys. Chem. Chem. Phys.*, 2020, **22**, 26876–26886.
24 S. Wurmehl, G. H. Fecher, K. Kroth, F. Kronast, H. A. Dürr, Y. Takeda, Y. Saitoh, K. Kobayashi, H. J. Lin, G. Schönhense and C. Felser, *J. Phys. D. Appl. Phys.*, 2006, **39**, 803–815.
25 S. Wurmehl, J. Morais, M. d. C. M. Alves, S. R. Teixeira, G. H. Fecher and C. Felser, *J. Alloys Compd.*, 2006, **423**, 159–162.
26 K. Inomata, N. Tezuka, S. Okamura, H. Kurebayashi and A. Hirohata, *J. Appl. Phys.*, 2004, **95**, 7234–7236.
27 K. Kobayashi, R. Y. Umetsu, R. Kainuma, K. Ishida, T. Oyamada, A. Fujita and K. Fukamichi, *Appl. Phys. Lett.*, 2004, **85**, 4684–4686.
28 J. Rodriguez-Carvajal, *Physica B*, 1993, **192**, 55.
29 H. T. Brian, *Powder Diffr.*, 2006, **21**(1), 67–70.
30 L. Bainsla, A. I. Mallick, M. M. Raja, A. A. Coelho, A. K. Nigam, D. D. Johnson, A. Alam and K. G. Suresh, *Phys. Rev. B: Condens. Matter Mater. Phys.*, 2015, **92**, 1–5.
31 C. C. Fu, M. Y. Lavrentiev, R. Soulairol, S. L. Dudarev and D. Nguyen-Manh, *Phys. Rev. B: Condens. Matter Mater. Phys.*, 2015, **91**, 1–16.
32 H. Yamamoto, *Jpn. J. Appl. Phys.*, 1964, **3**, 745–748.

33 R. K. Yadav, R. Govindaraj and G. Amarendra, *AIP Conf. Proc.*, 2020, **2220**, 110001–110004.
34 K. Özdogan, I. Galanakis, E. Şaşioglu and B. Aktaş, *Phys. Status Solidi Rapid Res. Lett.*, 2007, **1**, 95–97.
35 I. Galanakis, P. H. Dederichs and N. Papanikolaou, *Phys. Rev. B: Condens. Matter Mater. Phys.*, 2002, **66**, 1–9.
36 Y. Zhang, G. Wu, W. Zhu, Z. Ji, Q. Y. Jin and Z. Zhang, *Phys. Chem. Chem. Phys.*, 2021, **23**, 12612–12619.
37 S. V. Karthik, A. Rajanikanth, Y. K. Takahashi, T. Okhubo and K. Hono, *Appl. Phys. Lett.*, 2006, **89**, 2–5.
38 S. V. Karthik, A. Rajanikanth, T. M. Nakatani, Z. Gercsi, Y. K. Takahashi, T. Furubayashi, K. Inomata and K. Hono, *J. Appl. Phys.*, 2007, **102**, 1–7.
39 T. Block, C. Felser, G. Jakob, J. Ensling, B. Mühling, P. Gütlich and R. J. Cava, *J. Solid State Chem.*, 2003, **176**, 646–651.
40 V. N. Antonov, H. A. Dürr, Y. Kucherenko, L. V. Bekenov and A. N. Yaresko, *Phys. Rev. B: Condens. Matter Mater. Phys.*, 2005, **72**, 054441.
41 M. D. Mukadam, S. Roy, S. S. Meena, P. Bhatt and S. M. Yusuf, *Phys. Rev. B: Condens. Matter Mater. Phys.*, 2016, **94**, 214423.
42 F. Casper, T. Graf, S. Chadov, B. Balke and C. Felser, *Semicond. Sci. Technol.*, 2012, **6**, 27.
43 K. Elphik, W. Frost, M. Samiepour, T. Kubota, K. Takamashi and H. Sukegawa, *Sci. Technol. Adv. Mater.*, 2021, **22**, 235.
44 Enamullah, D. D. Johnson, K. G. Suresh and A. Alam, *Phys. Rev. B: Condens. Matter Mater. Phys.*, 2014, **94**, 18410.